

ORIGINAL ARTICLE

Anti-microbial, Anti-inflammatory and Anti-cancer Potentials of *Eobaniavermiculata* (Müller, 1774) Mucin-conjugated Gold Nanoparticles

¹Amina M. Ibrahim, ²Abdullah E. Gouda, ²Hend Okasha, ³Heba Dahroug*,
²Mohamed A. Shemis

¹Medical Malacology Department, Theodor Bilharz Research Institute, Giza, Egypt

²Biochemistry and Molecular Biology Department, Theodor Bilharz Research Institute, Giza, Egypt

³Microbiology Department, Theodor Bilharz Research Institute, Giza, Egypt

ABSTRACT

Key words:

Eobania vermiculata snails;
Mucin-conjugated gold
nanoparticles; Anticancer;
Anti-inflammatory;
Antibacterial activities

*Corresponding Author:

Heba Dahroug
Microbiology Department,
Theodor Bilharz Research
Institute, Giza, Egypt
Tel.: 01223722782
hubbymicro@yahoo.com

Background: Terrestrial snails produce slime with antimicrobial properties used in skincare products. Mucin, derived from snail mucus, has biomedical applications like wound healing and anti-cancer purposes. Mucins are glycosylated proteins used in fields like biotechnology. The Helix complex in mucin provides antibacterial and therapeutic benefits, including skin protection and wound repair. Snail mucin has anti-tumor activity against melanoma cells. Gold nanoparticles explored for drug delivery and wound healing. **Objective:** Research on mucin from *E. vermiculata* aims to assess anti-inflammatory, antimicrobial, and anti-cancer potentials for skincare and wound healing. **Methodology:** Slime was collected from snails and extracted to obtain mucin fraction. Gold nanoparticles were activated and incubated with mucin protein. The hydrodynamic diameter and zeta-potential of the nanoparticles were determined. A protein acrylamide gel was prepared to elucidate mucin conjugation. In vitro tests were conducted using different extracts and proteins to evaluate denaturation. A cytotoxicity assay using hemolysis and Vero cell line was performed to assess cellular toxicity. The anticancer activity of conjugated mucin on HepG2 cell line was evaluated. MIC were determined for various substances using bacterial isolates. The antimicrobial effect was examined on different Gram-negative bacteria. The minimum growth inhibitory concentration of ceftriaxone in free and nanostructure forms was determined using the broth dilution method. Statistical analysis was conducted to evaluate the results of the study. **Results:** The absorption and IR spectra indicated protein binding to AuNPs, confirmed by the presence of specific peaks related to peptides and amino acids. SDS-PAGE analysis verified the conjugation of mucin to AuNPs. Cytotoxicity evaluation showed minimal effects on membrane stabilization and hemolysis, with no cytotoxicity against normal kidney cells but significant anti-proliferative effects on liver cancer cells. Antimicrobial testing revealed improved efficacy against *E. coli* with conjugated mucin, while gold nanoparticles also exhibited antimicrobial effects. **Conclusion:** *E. vermiculata* mucin-AuNPs have antimicrobial, anti-inflammatory, anticancer effects.

INTRODUCTION

Terrestrial snails secrete slime¹, which protects the animal from microbial infections hence it was considered a powerful antimicrobial agent, and widely used in many skincare compositions and anti-aging formulas^{2,3}. Recently, a derivative of mucous called mucin has been widely used in biomedical applications as a wound healing, hepatoprotective, antioxidant, anticancer, anti-microbial agent, and the treatment of skin disturbances³. Mucins are a highly glycosylated protein family that were used as a lucrative agent in biotechnology, biomedicine, biology, and chemistry⁴. Where mucin-based films to polyethylene terephthalate

could effectively reduce the immune response triggered by IgG and IgM absorption into the plastic⁵.

Because of the presence of the Helix complex, which includes glycolic acid and allantoin, the mucin had antibacterial action as well as a number of therapeutic qualities, including skin protection and wound repair⁶. A study on *Helix aspersa maxima* snail's mucous confirmed the anti-tumor activity against human melanoma cells, where it declined the viability and hindered the metastasis of melanoma cells. Snail mucin biopolymers could be used as excellent candidates for novel medication delivery systems due to their flexibility. Gold nanoparticles have obtained great attention owing to their low toxicity to animal and

microorganism cells compared to other metal nanoparticles, thus supporting their use as drug delivery systems, markers, and photo-thermal agents, as well as radiotherapy enhancers⁷.

Recent studies have established new prospects for preparing well-functionalized AuNPs for wound healing. The AuNPs use should have profits including improved mechanical stability and resistance against enzymatic degradation when incorporated into tissue scaffolds for skin tissue engineering applications⁸. To try this paradigm, a snail secretion from *Helix aspersa*, has been used for synthesizing AuNPs, which are used in cosmetics and human skincare. The AuNPs-SS could be used as a wound healing and anti-inflammatory agent⁹.

In this study we aimed to investigate the potential anti-inflammatory, antimicrobial and anti-cancer activity of mucin purified from *E. vermiculata* mucous conjugated to chemically synthesized AuNPs.

METHODOLOGY

All authors confirm that all methods were performed in accordance with the relevant guidelines and regulations

Ethics approval and consent to participate:

The blood sample used in the study was obtained from an archived blood sample from a research project (ID: 17-2-12) supported by the Ministry of Scientific Research Egypt and the National Research Foundation South Africa, with Professor Mohamed Abbas Shemis as the principal investigator. Ethical approval and informed consent were obtained for the use of blood from healthy human donors.

Pure slime was collected by using a sterile wooden rod to rub on the muscular foot of the snail. About 100ml of crude slime from thirty snails was collected, then it was sterilized by filtering through 0.45- μ m filter¹⁰ and was kept in sterile containers for 12 h at 4 °C to be used for extraction of mucin. The precipitation was re-dissolved with Tris-HCl buffer and finally, mucin fraction was obtained.

Diclofenac sodium, ceftriaxone disodium, normal Saline, and ultra-pure water were kindly obtained from Pharco. This solution was heated for a further 10 min and then cooled to room temperature with continuous stirring. Finally, the resulting solution was filtered through a 0.2 μ m ultra-filtration membrane to remove aggregated particles and stored at 4°C^{11,12,13,14}. The precipitate was triplet-washed with water and centrifuged subsequently.

The washed gold nanoparticles (AuNPs) were synthesised from an aqueous solution of gold chloride (hydrogen tetrachloroaurate (III) trihydrate, HAuCl₄, with a concentration of 1.0 g/L.) Gold (III) chloride trihydrate (HAuCl₂) were supplied by Loba-chemi (India). were resuspended in ultra-pure water to a

concentration of 100 μ g/ ml. The resuspended particles were activated using 40 mM of EDC and 10 mM of NHS (N-Hydroxysuccinimide) were purchased from Sigma-Aldrich (Germany).and incubated for two hours with moderate stirring. Then, the lyophilized mucin protein was resuspended in both the activated gold nanoparticles solution and ultra-pure water to a concentration of 1 mg/ ml and incubated with AuNPs for 3 and 12 hours⁸.

The average hydrodynamic diameter and zeta-potential of AuNPs with and/ or mucin protein were determined with a particle size analyzer. The size and zeta potential measurements were carried out at 25°C in disposable size and zeta cuvettes with water as solvent¹⁰. The suspension of the material was sonicated for 20 minutes on an ultrasonicator. To elucidate the mucin conjugation to AuNPs an acrylamide gel was prepared. (The protein acrylamide gel contained two layers, the upper stacking gel was composed of 0.133% N, N-methylene bisacrylamide, 0.12 M Tris-HCl, 0.1% ammonium persulfate and 0.1% N, N, N', N'-tetramethylethylenediamine (TEMED). The lower separating gel was composed of 0.040% N, N-methylene bisacrylamide, 0.199 M Tris-HCl, 0.053 M SDS, 0.053% ammonium persulfate and 0.053% TEMED. Electrophoresis was carried out at a constant volt in an electrode buffer composed of 0.195 M glycine, 0.025 M Tris-HCl, and 0.1% SDS 35. Using the Coomassie staining technique, the gels were stained in a solution composed of 10% acetic acid, 40% methanol, and 0.2% Coomassie brilliant blue for 30-45 min. Different extracts against the denaturation of protein were *in vitro* tested using egg or bovine serum albumin^{15,16}

A 5ml solution was made which was comprised of 2.8ml of freshly prepared phosphate-buffered saline((137 mM NaCl, 10 mM phosphate, 2.7 mM KCl; pH 7.4), 2 ml of specific concentration of mucin, mucin-Au-NPs, and Au-NPs to which 0.2 ml of bovine serum albumin was added. Specific concentrations were prepared separately for mucin as 500 μ g/ml, 250 μ g/ml, 125 μ g/ml, 62.5 μ g/ml, 31.25 μ g/ml, 15.56 μ g/ml, and 7.78 μ g/ml. The same concentrations were prepared for the mucin-AuNPs along with 100 μ g/ml, 50 μ g/ml, 25 μ g/ml, 12.5 μ g/ml, 6.25 μ g/ml, and 3.125 μ g/ml for the AuNPs^{17,18}-respectively. Diclofenac sodium was used as the positive control with the same concentrations. Then the mixtures were heated in a water bath at 37°C for 20 minutes and the temperature was gradually increased up to 70°C at which the samples were kept for 5 minutes. When the drug is administrated and circulated into the bloodstream, RBCs appear to be the first biological moieties being affected¹⁶ The tubes were centrifuged at 3000 rpm for 10 minutes, then plasma was decanted and RBCs were washed three times with an equal volume of normal saline. Mucin was prepared in a variety of

concentrations, including 500 g/ml, 250 g/ml, 125 g/ml, 62.5 g/ml, 31.25 g/ml, 15.56 g/ml, and 7.78 g/ml. The same concentrations were prepared for the mucin-AuNPs along with 100 µg/ml, 50 µg/ml, 25 µg/ml, 12.5 µg/ml, 6.25 µg/ml, and 3.125 µg/ml for the AuNPs respectively. The percentage of hemolysis was estimated by assuming the hemolysis produced in the control as 100%.

The cytotoxicity assay involves using hemolysis as a rapid method to evaluate cellular toxicity, but results can vary depending on the methods and buffers used. Employing other cell types with standardized methods can provide a more accurate assessment of a compound's cytotoxicity^{19, 20}. Vero cell line was used in this study and was grown in MEM media with supplements. The cells were seeded in a 96-well plate and treated with different concentrations of test substances, including mucin, mucin-AuNPs, and AuNPs. Doxorubicin was used as a positive control. After incubation, the cells were washed and stained with crystal violet solution. The plates were washed and air-dried before adding methanol and measuring the optical density at 570 nm. The percentage viability was calculated using the formula % Viability = $(\text{Abs}_{\text{sample}} - \text{Abs}_{\text{blank}} / \text{Abs}_{\text{mc}} - \text{Abs}_{\text{blank}}) \times 100$. This assay provides valuable information on the cytotoxic effects of compounds on cells, helping researchers to assess the safety and effectiveness of potential treatments.

The study evaluated the anticancer activity of conjugated mucin on HepG2 cell line. The cells were cultured in RPMI-1640 medium with supplements and incubated to reach 70% confluence. Different concentrations of mucin, mucin-AuNPs, AuNPs, and Doxorubicin (positive control) were prepared and added to the cells. After 24 hours, the cells were stained with crystal violet solution, washed, dried, and incubated with methanol. The optical density of each well was measured at 590 nm to determine cell viability²¹.

The formula used to calculate the percentage viability of cells was % viability = $(\text{Abs}_{\text{sample}} - \text{Abs}_{\text{blank}} / \text{Abs}_{\text{mc}} - \text{Abs}_{\text{blank}}) \times 100$, where $\text{Abs}_{\text{sample}}$ is the absorbance of the sample, $\text{Abs}_{\text{blank}}$ is the absorbance of the blank, and Abs_{mc} is the absorbance of the control medium. This method allowed the researchers to assess the impact of mucin and its conjugates on the viability of HepG2 cells, providing valuable information on the potential anticancer activity of these substances.

The minimum inhibitory concentrations were determined for Ceftriaxone as a standard drug, Conjugated Mucin, free Mucin, and free AuNP

using two-fold dilution starting from 100 µg/ml. The antimicrobial effect was examined using five different bacterial isolates *Klebsiella pneumoniae*, *Proteus mirabilis*, *Morganellamorganii*, *Escherichia coli*, and *Pseudomonas aeruginosa*. Using a sterile microdilution plate with conical bottom wells, 50 µl of each concentration of the tested sample was mixed with 50 of the bacterial isolate. The antimicrobial effect was examined on five different Gram-negative bacterial isolates namely *Klebsiella pneumoniae*, *Proteus mirabilis*, *Morganella morganii*, *Escherichia coli*, and *Pseudomonas aeruginosa*²². (Our isolates were tested against quality control strains *Escherichia coli* ATCC 25922, *Pseudomonas aeruginosa* ATCC 27853, *Klebsiella pneumoniae* ATCC 700603, *Proteus mirabilis* ATCC 35659, ATCC25830). To determine the minimum growth inhibitory concentration of ceftriaxone in free and nanostructure forms, the broth dilution method was used under Clinical and Laboratory Standard Institute guidelines²³. Two fold serial dilution was used from 128 µg/ml to 0.0078 µg/ml and a tube as the positive control. We prepared a 24h bacterial culture in a sterile suspension physiological serum equivalent to 0.5 McFarland standard turbidity. The culture was followed by incubation of media containing antibiotics, which were then transferred to a 35R oven and remained there for 24 h to grow completely. After 24 h, tubes were examined bacterial growth. The minimum concentration of bacteria without visible growth was considered MIC.

Statistical analysis

The data were presented as the mean ± SD. The test of significance was performed by Graph Pad Prism 8 (San Diego, California, USA) using paired T-test and two-way ANOVA. The $p < 0.001$ was considered a high statistically significant difference.

RESULTS

The AuNPs-mucin conjugation process involved the synthesis of AuNPs, characterized by color change and DLS. The resulting AuNPs had different sizes and surface charges depending on the incubation period, showing a narrow size distribution. The AuNPs-p2 variant had the largest size and least negative surface charge. Characterization was done using DLS, Polydispersity index, and zeta potential analysis.

(Fig.1a, b& c), and a surface charge of -24.91 ± 1.57 , -22.97 ± 1.65 and -14.61 ± 1.44 mV respectively (Fig.1.d, e& f).

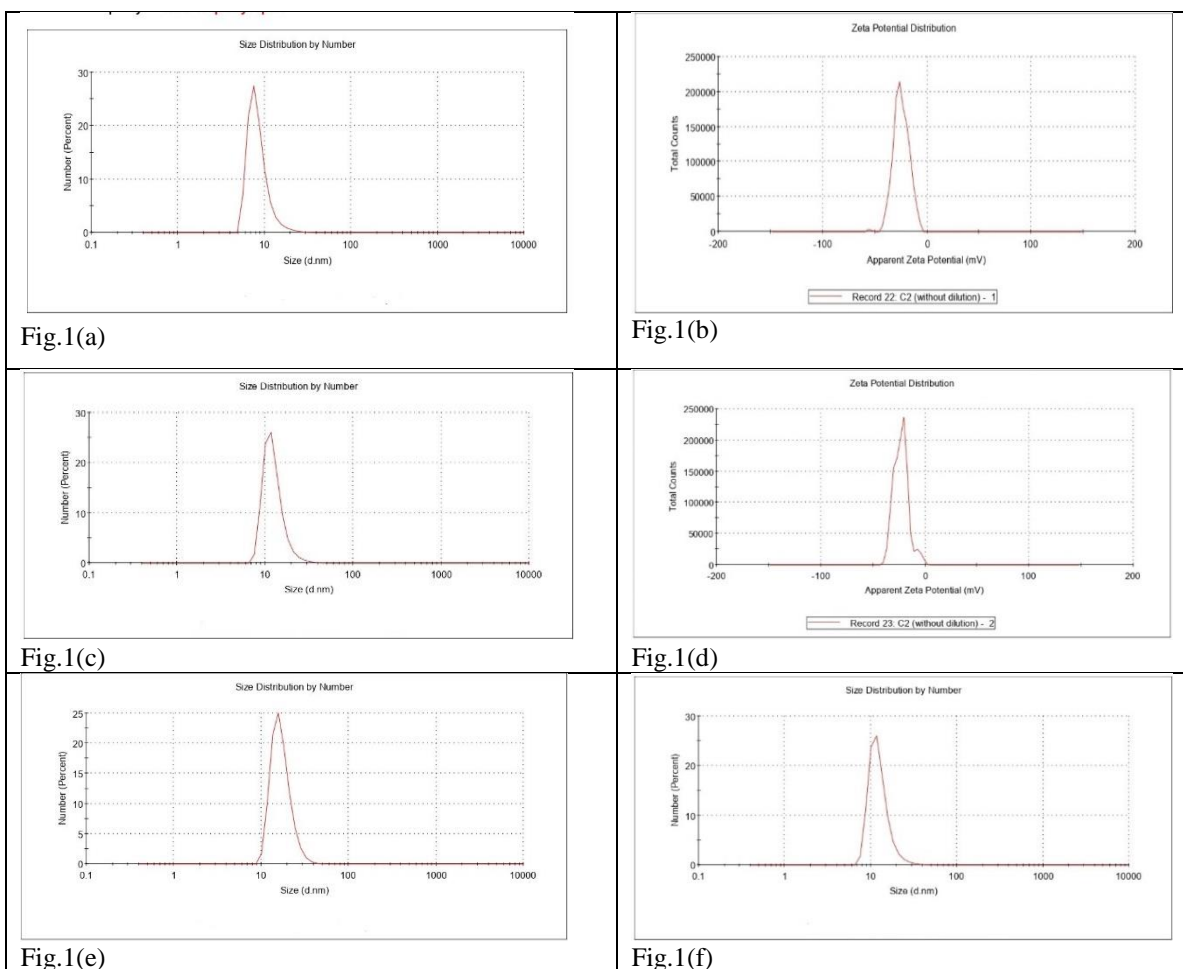


Fig.1: (a, b &c) size distribution (nm), (d, e& f) zeta potential of AuNPs (mV) of AuNPs, AuNPs-p1 & AuNPs-p2 respectively.

The results of the transmission electron microscopy confirmed the nano-metric size and the spherical morphology of the prepared empty AuNPs (10.48 ± 1.14 nm) conjugated AuNP-P1 (10.77 ± 1.39 nm) and AuNPs-P2 (14.13 ± 2.94 nm). All AuNPs attained

spherical shape with an inner dark portion of goldcapped in a citrate shell, which is surrounded by the outer smooth layers of mucin protein that stabilizes the particles from aggregation and all nanoparticles maintained amorphous structure as shown in fig. 3.

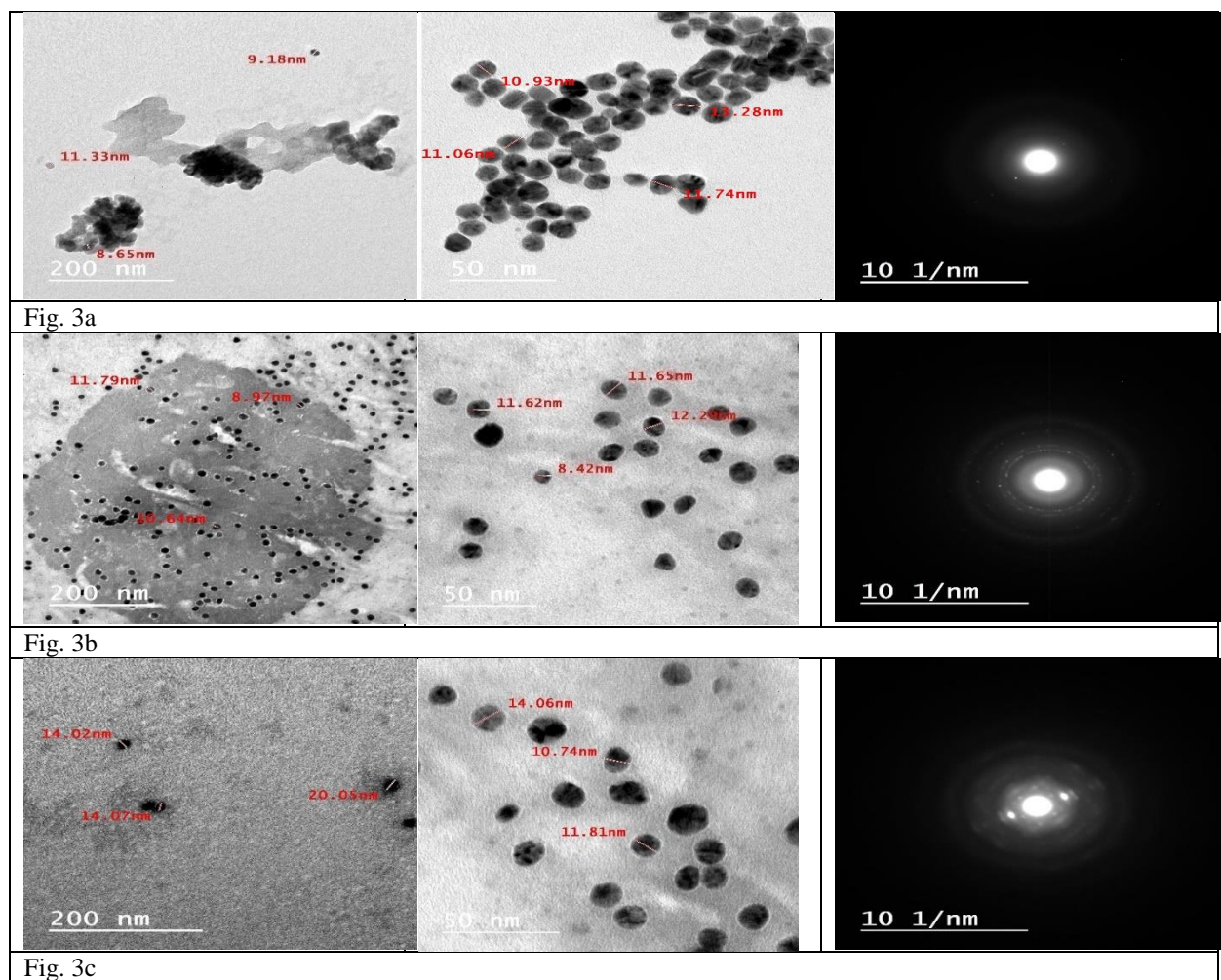


Fig.3: (a) Representative TEM images of unconjugated AuNPs, (b & c) TEM images of mucin conjugated AuNPs (AuNPs-p1 & AuNPs-p2 respectively).

The absorption spectra of AuNPs change when proteins bind to them, as shown by a visible shift in wavelength and a decrease in peak intensity. The IR spectra of the conjugated AuNPs revealed distinct peaks corresponding to different vibrations, such as COO-stretching and sp³ C-H stretching. The presence of peaks related to N-H stretching and O-H stretching

indicated the presence of peptides or amino acids on the AuNPs' surface. The conjugation of mucin protein to AuNPs was confirmed through SDS-PAGE, showing a larger band for the mucin-AuNP conjugate compared to free mucin. The amount of mucin protein conjugated to the AuNPs was determined to be 5 µg/ml. (Table 1).

Table1: The percent Inhibition of protein denaturation treated with mucin, mucin-Au-NPs, AuNPs & Diclofenac sodium

| Serial dilution (µg/ml) | % Inhibition | | | |
|----------------------------|--|-------------|-------|-------------------|
| | Mucin | mucin-AuNPs | AuNPs | Diclofenac sodium |
| 500:100 | 50.10 | 61.38 | 57.43 | 68.36 |
| 250: 50 | 42.81 | 50.10 | 48.17 | 55.29 |
| 125: 25 | 33.82 | 47.75 | 42.08 | 50.24 |
| 62.5: 12.5 | 21.13 | 40.59 | 36.62 | 41.63 |
| 31.25:6.25 | 17.46 | 34.16 | 32.16 | 36.07 |
| 15.56:3.12 | 13.62 | 19.99 | 14.25 | 23.82 |
| 7.78:1.56 | 7.88 | 15.94 | 13.17 | 19.47 |
| N.B. | for example, 500:100 means that 500 µg of mucin conjugate to 100 µg GNPs | | | |

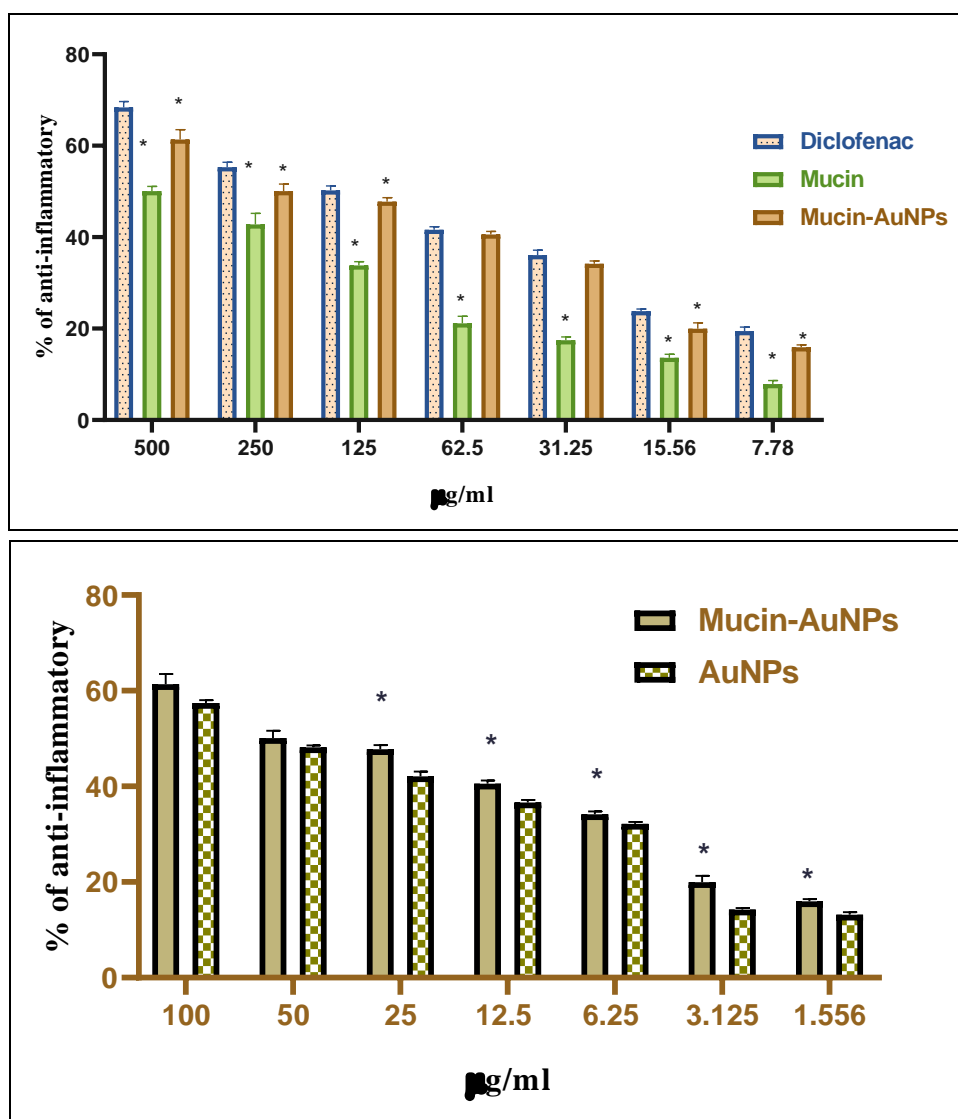


Fig.4: The percent inhibition of protein denaturation treated with mucin, mucin-Au-NPs, AuNPs & Diclofenac sodium. The evaluation of cytotoxic activity of conjugated mucin, snail mucin, mucin-AuNPs, and AuNPs had a slight effect on membrane stabilization. Conjugation of snail mucin to gold nanoparticles did not increase hemolysis of red blood cells, with hemolysis maintained below 10% even at maximum concentrations. Table(2). Paired T-test between mucin-AuNPs and AuNPs showed a significant correlation (p -value= 0.022). Two novel tryptophan-based ionic liquids with the tryptophan (Trp) group acting as a reducing agent were used to create AuNPs with a variety of forms, sizes, and zeta potentials. According to the hemolysis % results, AuNPs are extremely biocompatible.

Table 2: The percent hemolysis of RBCs treated with mucin, mucin-Au-NPs, and AuNPs

| Serial dilution (µg/ml) | Hemolysis | | |
|-------------------------|-----------|-------------|--------|
| | Mucin | Mucin-AuNPs | AuNPs |
| 500:100 | 9.684% | 9.295% | 9.998% |
| 250: 50 | 8.299% | 8.332% | 8.905% |
| 125: 25 | 7.131% | 7.228% | 7.704% |
| 62.5: 12.5 | 6.709% | 6.092% | 6.871% |
| 31.25:6.25 | 5.388% | 5.832% | 5.713% |
| 15.56:3.12 | 4.101% | 3.971% | 4.198% |
| 7.78:1.56 | 3.257% | 3.387% | 3.473% |

Cytotoxicity assay:

The cytotoxic effect of mucin, mucin-AuNPs, and AuNPs and standard (Doxorubicin) was evaluated *in vitro* against Vero normal kidney cell lines after 24 h exposure. The results showed no cytotoxic effect over the different ranges varying from 7.78 µg/ml to 500 µg/ml compared to the common anticancer drug, Doxorubicin as cytotoxic control. One-way ANOVA revealed a statistical significance (p -value= 0.0154) between reference drug DOX, mucin-Au-NPs, and AuNPs. Res

Evaluation of the anticancer activity of conjugated mucin:

The results of the anticancer activity on the liver cancer HepG2 cell line showed that the mucin, mucin-AuNPs, AuNPs & doxorubicin (positive control) have revealed well anti-proliferative activity against the cancer cell line. All the tested materials proved to be efficient in most of the concentrations tested and the inhibition concentration of 50 (IC_{50}) was 87.5 µg/ml for mucin, 52 µg/ml for mucin-AuNPs, 11.8 µg/ml for AuNPs, and 2.2 for DOX with high statistical significance (p -value< 0.0001).

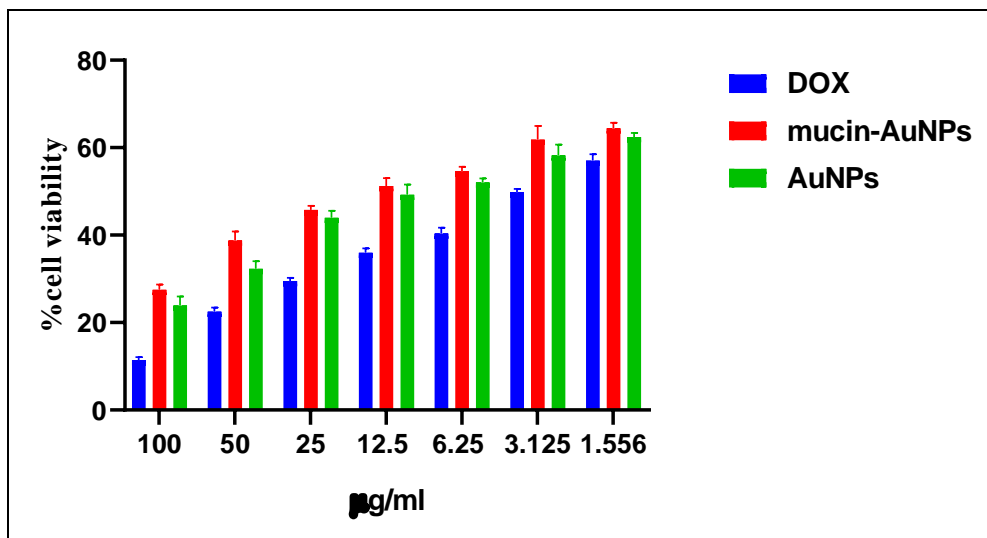


Fig. 5: The percent Viability of HepG2 cell lines treated with mucin, mucin-AuNPs, AuNPs & doxorubicin. Each sample was repeated three times and the mean with SD was plotted (p -value< 0.0001).

- Antimicrobial susceptibility testing:

Conjugated mucin revealed better antimicrobial efficacy when tested in *E.coli* isolate with a reduction from 7.03 µg/ml with free mucin to 2.9 µg/ml with conjugated mucin. However, in *Morganella morganii* isolate the effect of free mucin recorded a lower MIC of 7.5 µg/ml than conjugated mucin at 10.5 µg/ml. No antibacterial effect was detected against the remaining isolates which may be attributed to the antibacterial activity of mucin either free or conjugated associated

with characteristics of certain bacterial isolates. Compared to mucin and conjugated mucin the effect of gold nanoparticles was studied. It was found that MICs of isolates 1,2 and 4 with free gold nanoparticles reduced significantly compared to their free forms. The lowest MIC was detected at 0.468 µg/ml and 0.99 µg/ml for *Morganella morganii* and *E. coli*, respectively, while *K. pneumonia* was less sensitive and its MIC reached 2.1 µg/ml (Table 3).

Table 3: MICs (µg/ml) of Ceftriaxone (Rx), Conjugated Mucin, free Mucin, and free AuNP in different bacterial isolates (p -value = 0.0017)

| | Ceftriaxone (Rx) | Conjugated Mucin | Free Mucin | Free AuNP |
|---------------------------------------|------------------|------------------|------------|------------|
| Isolate 1: <i>E.coli</i> | 21.89±1.6 | 27.82±1.9 | 29.78±3.1 | 2.11±0.99 |
| Isolate 2: <i>P.aeruginosa</i> | 21.77±1.04 | 10.5±1.3 | 7.4±2.6 | 0.47±0.17 |
| Isolate 3: <i>Morganella</i> | 2.33±0.33 | 335.5±25.2 | 489.5±50.4 | 48.43±5.15 |
| Isolate 4: <i>K.pneumonia</i> | 1.714±0.22 | 2.9±1.6 | 7.03±1.55 | 0.99±0.7 |
| Isolate 5: <i>Proteus</i> | 2.52±0.47 | 18.65±2.4 | 10.74±1.99 | 31.95±2.7 |

DISCUSSION

The current Study examines anti-inflammatory, antimicrobial, anti-cancer properties of *E. vermiculata* mucin conjugated to AuNPs. Protein binding to AuNP alters the absorption spectra of the particles, which is in line with reported results by Chang et al. and Jelen et al.,^{12,13} who observed shifts in peak maximum when different proteins were bound to AuNPs.^{24,25}

The study utilized an ATR-IR approach to measure IR spectra of purified citrate-coated AuNPs. Differences in peak positions were noted between pure AuNPs and AuNPs conjugated with mucin protein, indicating successful conjugation. Peaks corresponding to N-H stretching and O-H stretching vibrations suggested the presence of peptides or amino acids on the surface of the AuNPs. Overall, the ATR-IR results confirmed the successful conjugation of mucin protein to the AuNPs, consistent with previous research findings.^{11,25,26}

The results of this study indicate that the conjugation of snail mucin to gold nanoparticles enhances its anti-inflammatory activity. Results showed that these compounds effectively inhibited heat-induced albumin denaturation in a concentration-dependent manner. The IC₅₀ values for mucin, mucin-AuNPs, AuNPs, and the standard diclofenac sodium were determined, with AuNPs demonstrating the highest efficacy at 82.5 µg/ml. These results are in agreement with the study published by (27), which reported the IC₅₀ of AuNPs to be 87.5 µg/ml. The anti-inflammatory activity of mucin purified from *Eobania vermiculata* outperforms the anti-inflammatory activity of the slime extracts from the giant African snail, *Lissachatina fulica*. These findings suggest the potential of mucin and AuNPs for controlling inflammation through protein denaturation inhibition.

Our study found that snail mucin, mucin-AuNPs, and AuNPs had a slight effect on membrane stabilization, with no significant increase in hemolysis of red blood cells even at high concentrations. The results were consistent with previous studies on hemolytic effects of aqueous and ethanolic slime extracts.²⁸ A paired T-test showed a significant correlation between mucin-AuNPs and AuNPs. Other research has shown that coated and uncoated AuNPs did not trigger osmotic hemolysis or cause erythrocyte hemolysis in vitro.²⁹ Different sizes of AuNPs were found to have varying effects on hemolysis, with smaller sizes promoting modest hemolysis. Additionally, studies on tryptophan-based ionic liquids and AuNPs showed that AuNPs are highly biocompatible and have no adverse effects on red blood cell morphology or hemoglobin structure. Furthermore, the study observed differences in cellular absorption of different types of coated AuNPs by leukocytes and platelets.³⁰

The study evaluated the cytotoxic effect of mucin, mucin-AuNPs, and AuNPs on Vero normal kidney cell lines, showing no cytotoxicity compared to Doxorubicin. One-way ANOVA indicated a statistical significance between Doxorubicin, mucin-Au-NPs, and AuNPs.⁹ The conjugation of mucin-AuNPs did not induce cytotoxic activity, and AuNPs-mucin treatment increased uPAR levels, suggesting wound healing acceleration. In another study, the effects of *Eremina desertorum* and *Helix aspersa* snail mucus on HSF normal cells were assessed, showing no cytotoxicity. At the highest concentration (300 µg/ml), cell viability was 93% for *H. aspersa* and 75.8% for *E. desertorum*, with IC₅₀>300 µg/ml confirming no toxic effects.¹⁰

Both AuNPs prepared by biosynthesis have a slightly lower anticancer effect than those prepared by chemical synthesis in this study. Another previous study used gold Nanoclusters embedded mucin nanoparticles for photodynamic therapy and imaging through the delivery of methylene blue. The cell viability assay revealed that the viability of HeLa cancer cells was reduced to 50 % after treatment with the biocompatible MB-loaded Au NCs-mucin NPs. AuNPs are most promising due to their excellent optical and photoelectric properties, inertness, no toxicity, higher stability, ease of preparation, and the possibility of bioconjugation.³¹

The results of MICs suggested that AuNPs can be used to control pathogenic bacterial growth. AuNPs act on bacteria through preventing the uncoiling of DNA by binding to the DNA and lead to inhibit the transcription process, which leads to cell death.^{32,33} In the same manner, MIC of gold nanoparticles was determined against all selected Gram-negative isolates, this method represents the actual amount of AuNPs required to inhibit bacterial growth that can be determined and not estimated.³⁴ Based on the enhanced toxicity of AuNPs to bacterial cells, the study hypothesized that the cationic hydrophobic AuNPs particularly act on the integrity of bacterial membranes.³⁵ Moreover, AuNPs are able to disrupt the integrity of the bacterial membrane by electrostatic interaction. Our MIC data demonstrated that free AuNPs were significantly more effective at lower amounts than free CTX, mucin, and conjugated mucin against the aforementioned bacterial species.

Although AuNPs conjugated to mucin showed promising anti-inflammatory, antibacterial and anticancer effects; study have some limitations as, this is a complete in vitro study. Still, in vivo studies are further required to see its potency on animal models

CONCLUSION

The integration of nanotechnology in healthcare holds promise for the future, with challenges surrounding

nanoparticle manufacturing at scale. Snail mucin conjugated with gold nanoparticles offers potential for medical and biomedical applications, enhancing bioavailability. Gold nanoparticles combined with mucin effectively modulate inflammation, inhibit liver cancer cell proliferation, and outperform other materials in combating pathogens. This research suggests a promising path for addressing inflammation, cancer, and bacterial infections.

Conflicts of interest:

The authors declared that they have no competing interests

Availability of data and material:

All data generated or analyzed during this study are included in this published article.

REFERENCES

- Atta, S. A., Ibrahim, A. M. & Megahed, F. A. K. In-Vitro Anticancer and Antioxidant Activities of *Eremina desertorum* (Forsskal, 1775) Snail Mucin. *Asian Pac. J. Cancer Prev.* (2021) **22**, 3467–3474.
- Kostadinova, N. et al. Antioxidative screening of fractions from the mucus of garden snail *Cornu aspersum*. *Bulg. Chem. Commun.* (2018) **50**, 176–183..
- Abd El Azeem, H., Osman, G., El-sabbagh, S., & Sheir, S.. Antibacterial activity of some terrestrial gastropods from Egypt against *Staphylococcus aureus* and *Escherichia coli*. *Egy J Zoology*, (2020) **74**, 1-12.
- McDermott, M., Cerullo, A. R., Parziale, J., Achrak, E., Sultana, S., Ferd, J., ... & Holford, M.. Advancing discovery of snail mucins function and application. *Frontiers in bioengineering and biotechnology*, (2021) **9**, 734023.
- Silva, G. G., da Costa Valente, M. L., Bachmann, L., & Dos Reis, A. C.. Use of polyethylene terephthalate as a prosthetic component in the prosthesis on an overdenture implant. *Materials Science and Engineering: C*, (2019) **99**, 1341-1349.
- Ellijimi, C., Hammouda, M. B., Othman, H., Moslah, W., Jebali, J., Mabrouk, H. B., ... & Srairi-Abid, N. , *Helix aspersa maxima* mucus exhibits antimelanogenic and antitumoral effects against melanoma cells. *Biomedicine & Pharmacotherapy*, (2018),**101**, 871-880.
- Liu, H., Zhang, M., Meng, F., Su, C., & Li, J. . Polysaccharide-based gold nanomaterials: Synthesis mechanism, polysaccharide structure-effect, and anticancer activity. *Carbohydrate Polymers*, (2023)**121284**.
- Khan, F. A., Albalawi, R., & Pottoo, F. H.,Trends in targeted delivery of nanomaterials in colon cancer diagnosis and treatment. *Medicinal research reviews*, (2022),**42**(1), 227-258.
- Radwan, M. A., Essawy, A. E., Abdelmeguid, N. E., Hamed, S. S. & Ahmed, A. E. Biochemical and histochemical studies on the digestive gland of *Eobania vermiculata* snails treated with carbamate pesticides. *Pestic. Biochem. Physiol* (2008), **90**, 154–167.
- Chang, C. C., Wei, S. C., Wu, T. H., Lee, C. H. & Lin, C. W Aptamer-based colorimetric detection of platelet-derived growth factor using unmodified gold nanoparticles. *Biosens. Bioelectron*, (2013),**42**, 119–123 .
- Park, J.-W., & Shumaker-Parry, J. S. Structural Study of Citrate Layers on Gold Nanoparticles: Role of Intermolecular Interactions in Stabilizing Nanoparticles. *Journal of the American Chemical Society*, (2014), **136**(5), 1907–1921. doi:10.1021/ja4097384
- Chang, C. C., Wei, S. C., Wu, T. H., Lee, C. H., & Lin, C. W. Aptamer-based colorimetric detection of platelet-derived growth factor using unmodified gold nanoparticles. *Biosensors & bioelectronics*, (2012),**42**, 119-123. <https://doi.org/10.1016/j.bios.2012.10.072>
- Jelen Ž, Kovač J, Rudolf R. Study of Gold Nanoparticles Conjugated with SARS-CoV-2 S1 Spike Protein Fragments. *Nanomaterials*. 2023 Jul 25;**13**(15):2160. <https://doi.org/10.3390/nano13152160>
- Oliveira, A.E.F.; Pereira, A.C.; Resende, M.A.C.; Ferreira, L.F. Gold Nanoparticles: A Didactic Step-by-Step of the Synthesis Using the Turkevich Method, Mechanisms, and Characterizations. *Analytica* ,(2023), **4**, 250-263. <https://doi.org/10.3390/analytica4020020>
- Sambrook, J. & Russell, D. W. *Molecular cloning: a laboratory manual*. Cold Spring Harb. NY Cold Spring Harb. Lab. (2001) **1**, 112 .
- Okasha, H., Samir, S. & Nasr, S. M. Purified recombinant human Chromogranin A N46 peptide with remarkable anticancer effect on human colon cancer cells. *Bioorg. Chem.* (2021),**115**, 105266.
- Sarveswaran, R., Banukie Jayasuriya, W. & J A B N, J. W. In vitro assays to investigate the anti-inflammatory activity of herbal extracts: A Review Hypoglycaemic and antiinflammatory of *Pleurotus mushrooms* View project IN VITRO ASSAYS TO INVESTIGATE THE ANTI-INFLAMMATORY ACTIVITY OF HERBAL EXTRACTS: A REVIEW. *Jayasuriya al. World J. Pharm. Res* (2021),**6**, 131 .

18. Heendeniya, S. N., Ratnasooriya, W. D. & Pathirana, R. N. In vitro investigation of anti-inflammatory activity and evaluation of phytochemical profile of *Syzygium caryophyllatum*. ~ 1759 ~ J. Pharmacogn. Phytochem.(2021),7, 1759–1763 .
19. Okasha, H., Samir, S. & Nasr, S. M. Purified recombinant human Chromogranin A N46 peptide with remarkable anticancer effect on human colon cancer cells. *Bioorg. Chem.*(2021), **115**, 105266 .
20. Abdelmonsef, A. H. et al. A search for antiinflammatory therapies: Synthesis, in silico investigation of the mode of action, and in vitro analyses of new quinazolin-2,4-dione derivatives targeting phosphodiesterase-4 enzyme. *J. Heterocycl. Chem.* (2021) doi:10.1002/jhet.4395.
21. Luna-Vázquez-Gómez R, Arellano-García ME, García-Ramos JC, Radilla-Chávez P, Salas-Vargas DS, Casillas-Figueroa F, Ruiz-Ruiz B, Bogdanchikova N, Pestryakov A. Hemolysis of human erythrocytes by Argovit™ AgNPs from healthy and diabetic donors: An in vitro study. *Materials*. 2021;14(11):2792.
22. Svenson J, Stensen W, Brandsdal BO, Haug BE, Monrad J, Svendsen JS. Antimicrobial peptides with stability toward tryptic degradation. *Biochemistry*. 2008 ;47(12):3777-88.
23. Ebrahimi, S., Farhadian, N., Karimi, M. & Ebrahimi, M. Enhanced bactericidal effect of ceftriaxone drug encapsulated in nanostructured lipid carrier against gram-negative *Escherichia coli* bacteria: Drug formulation, optimization, and cell culture study. *Antimicrob. Resist. Infect. Control* (2020), **9**.
24. Wiya, C., Nantarat, N. & Saenphet, K. Antiinflammatory Activity of Slime Extract from Giant African Snail (*Lissachatina fulica*). *Indian J. Pharm. Sci.*(2020), **82**, 499–505 .
25. Pourali P, Dzmirutuk V, Pátek M, Neuhöferová E, Svoboda M, Benson V. Fate of the capping agent of biologically produced gold nanoparticles and adsorption of enzymes onto their surface. *Scientific Reports*. 2023 ;13(1):4916. <https://doi.org/10.1038/s41598-023-31792-5>
26. Caruso F, Furlong DN, Ariga K, Ichinose I, Kunitake T. Characterization of polyelectrolyte–protein multilayer films by atomic force microscopy, scanning electron microscopy, and Fourier transform infrared reflection–absorption spectroscopy. *Langmuir*. 1998 ;14(16):4559-65.
27. Priya MR K, Iyer PR. Antiproliferative effects on tumor cells of the synthesized gold nanoparticles against Hep2 liver cancer cell line. *Egyptian Liver Journal*. 2020 ;10:1-2.
28. Kozłowski R, Ragupathi A, Dyer RB. Characterizing the surface coverage of protein–gold nanoparticle bioconjugates. *Bioconjugate chemistry*. 2018 ;29(8):2691-700.
29. Uzma M, Prasad D, Sunayana N, Vinay R, Shilpashree H. Studies of in vitro antioxidant and anti-inflammatory activities of gold nanoparticles biosynthesised from a medicinal plant, *Commiphora wightii*. *Mater. Technol.* 2022 ;37(9):915-25.
30. Aseichev AV, Azizova OA, Beckman EM, Skotnikova OI, Dudnik LB, Shcheglovitova ON, Sergienko VI. Effects of gold nanoparticles on erythrocyte hemolysis. *Bulletin of experimental biology and medicine*. 2014 ;156(4):495-8.
31. Dutta D, Sailapu SK, Simon AT, Ghosh SS, Chattopadhyay A. Gold-nanocluster-embedded mucin nanoparticles for photodynamic therapy and bioimaging. *Langmuir*. 2019 ;35(32):10475-83.
32. Rai A, Prabhune A, Perry CC. Antibiotic mediated synthesis of gold nanoparticles with potent antimicrobial activity and their application in antimicrobial coatings. *Journal of Materials Chemistry*. 2010;20(32):6789-98.
33. Tao C. Antimicrobial activity and toxicity of gold nanoparticles: research progress, challenges and prospects. *Letters in applied microbiology*. 2018;67(6):537-43.
34. Yu Z, Li Q, Wang J, Yu Y, Wang Y, Zhou Q, Li P. Reactive oxygen species-related nanoparticle toxicity in the biomedical field. *Nanoscale research letters*. 2020 ;15(1):115.
35. Joshi AS, Singh P, Mijakovic I. Interactions of gold and silver nanoparticles with bacterial biofilms: Molecular interactions behind inhibition and resistance. *International Journal of Molecular Sciences*. 2020; (20):7658.